Supplementary Materials

Supplementary Table 1: Bacterial Strains and Growth Media

Strain	Growth Media
B. cepecia	Cation-adjusted Mueller-Hinton Broth II
E. coli WT BW25113	Luria Broth
E. coli CFT073	Luria Broth
C. difficile	Reinforced Clostridial Medium
P. acnes	Reinforced Clostridial Medium
H. influenza	Cation-adjusted Mueller-Hinton Broth II
V. cholerae	Luria Broth
A. baumannii AB17978	Luria Broth
A. baumannii AB5075	Luria Broth
E. coli UPEC CFT073	Gutnick Minimal Media
E. coli UPEC J96	Gutnick Minimal Media
E. coli BW25113	Gutnick Minimal Media
E. coli NCM3722	Gutnick Minimal Media
S. aureus MRSA COL	Luria Broth
S. aureus MRSA USA300	Luria Broth
M. fortuitum	Cation-adjusted Mueller-Hinton Broth II
N. gonorrhoeae	Cation-adjusted Mueller-Hinton Broth II
S. aureus VanA	Cation-adjusted Mueller-Hinton Broth II
S. aureus VISA	Cation-adjusted Mueller-Hinton Broth II
S. aureus MRSE	Cation-adjusted Mueller-Hinton Broth II
S. epidermidis	Cation-adjusted Mueller-Hinton Broth II
B. subtilis W168	Luria Broth
E. coli lptD4213	Luria Broth
E. faecium	Cation-adjusted Mueller-Hinton Broth II

S. pneumoniae	Cation-adjusted Muller-Hinton Broth II with 5% lysed horse blood

Supplementary Table 2: The 14 features evaluated in BCP analysis

Features of BCP Analysis
Cell Area
Cell Length
Cell Width
Cell Eccentricity
Cell Perimeter
Nucleoid Area
Ratio of Nucleoid to Cell
Nucleoid Eccentricity
DNA Length
DNA Width
DNA Perimeter
Mean Sytox intensity
Mean FM4-64 intensity
Mean Dapi intensity

Supplementary Figure Legends

Figure S1. SCH-79797 is bactericidal against *S. aureus*. Colony forming units (CFU ml^{-1}) after 3-hour treatment of *S. aureus* MRSA USA300 with 1% DMSO, 1X MIC SCH-79797 and 5X MIC novobiocin. Each data point represents 3 independent samples and 3 technical replicates. Mean ± s.d. are shown.

Figure S2. SCH-79797 is an effective antibiotic in an infection model of *G. mellonella* by *A. baumannii.* A-B. The percent survival of non-infected *G. mellonella* wax worms after treatment with 2µl/larva of 100% DMSO, 67µg/larva SCH-79797, 6µg/larva gentamicin, and

67μg/larva rifampicin. Data in (A) represents a typical cohort (n = 12) from a biological triplicate and the pooled results are presented in (B). Mantel-cox statistics for the cohort were calculated with PRISM. C. The percent survival of *A. baumannii* infected *G. mellonella* wax worms after treatment with 67μg/larva SCH-79797, 6μg/larva gentamicin, and 67μg/larva rifampicin. Data represents the pooled results from a biological triplicate. D. The average survival of drug-treated *A. baumannii* infected *G. mellonella* wax worms relative to larvae treated with DMSO. Data represents the pooled results from a biological triplicate.

Figure S3. SCH-79797 is not prone to resistance in both *S. aureus* and *A. baumannii*. A. Fold increase in resistance of *S. aureus* MRSA USA300 to SCH-79797, novobiocin, trimethoprim, and nisin after 25 days of serial passaging in 0.5X MIC of each drug and plotted on a log2 scale. Resistance was confirmed by remeasuring MIC's from aliquots of each passage that were collected and stored at -80^{o}C. B. Fold increase in resistance of *A. baumannii* AB17978 to SCH-79797 and gentamicin after 5 days of serial passaging in 0.5X MIC of each drug and plotted on a log2 scale. Resistance was confirmed as described above. The experiment was performed in duplicate and identical results were found in both cases.

Figure S4. Thermal stability of DHFR increases after SCH-79797 and Trimethoprim treatment. A-B. The relative thermal stability of DHFR after treatment of whole cell and cell lysate samples with (A) SCH-79797 and (B) trimethoprim. Changes in thermal stability were determined by measuring changes in the abundance of DHFR across 10 different temperatures ranging from 42-72^{o}C and 4 drug concentrations and a vehicle control.

Figure S5. CRISPRi mutants not involved in folate metabolism are not sensitized to SCH-79797. A. The growth of CRISPRi *B. subtilis* knockdown mutants relative to a DMSO-treated control after SCH-79797 treatment. Bacterial growth was measured for 14h and the final optical density (OD600) of each condition was plotted against drug concentration. Each data point represents 2 independent replicates. Mean ± s.d. are shown.

Figure S6. Treatment with ampicillin, rifampicin, and novobiocin does not disrupt membrane integrity. A. Flow cytometry analysis of the membrane potential and permeability of *E. coli* lptD4213 cells after 15 min. incubation with 2X MIC ampicillin, rifampicin, novobiocin.

Figure S7. SCH-79797 disrupts *B. subtilis* W168 membrane integrity. A. Flow cytometry analysis of the membrane potential and permeability of *B. subtilis* W168 cells after 15 min. incubation with 1% DMSO, 1X MIC SCH-79797, 2X MIC SCH-79797.

Supplementary Figure 1

A

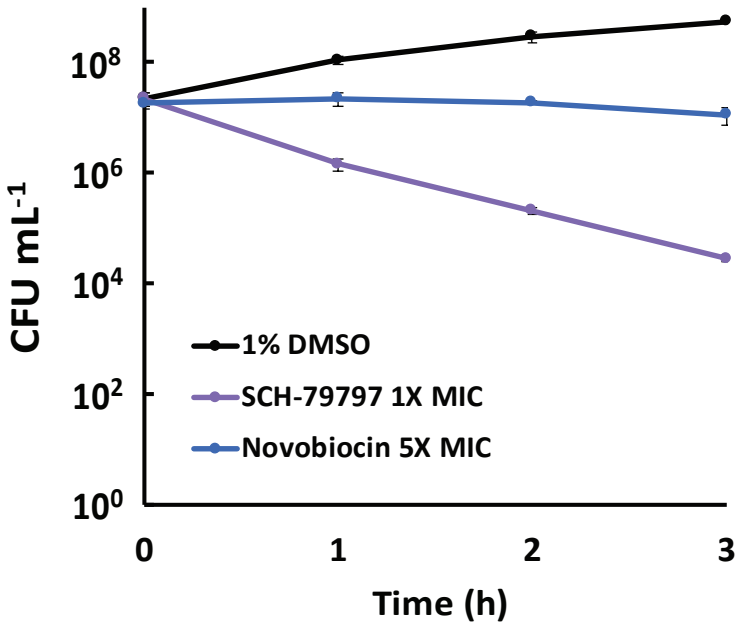

Supplementary Figure 2

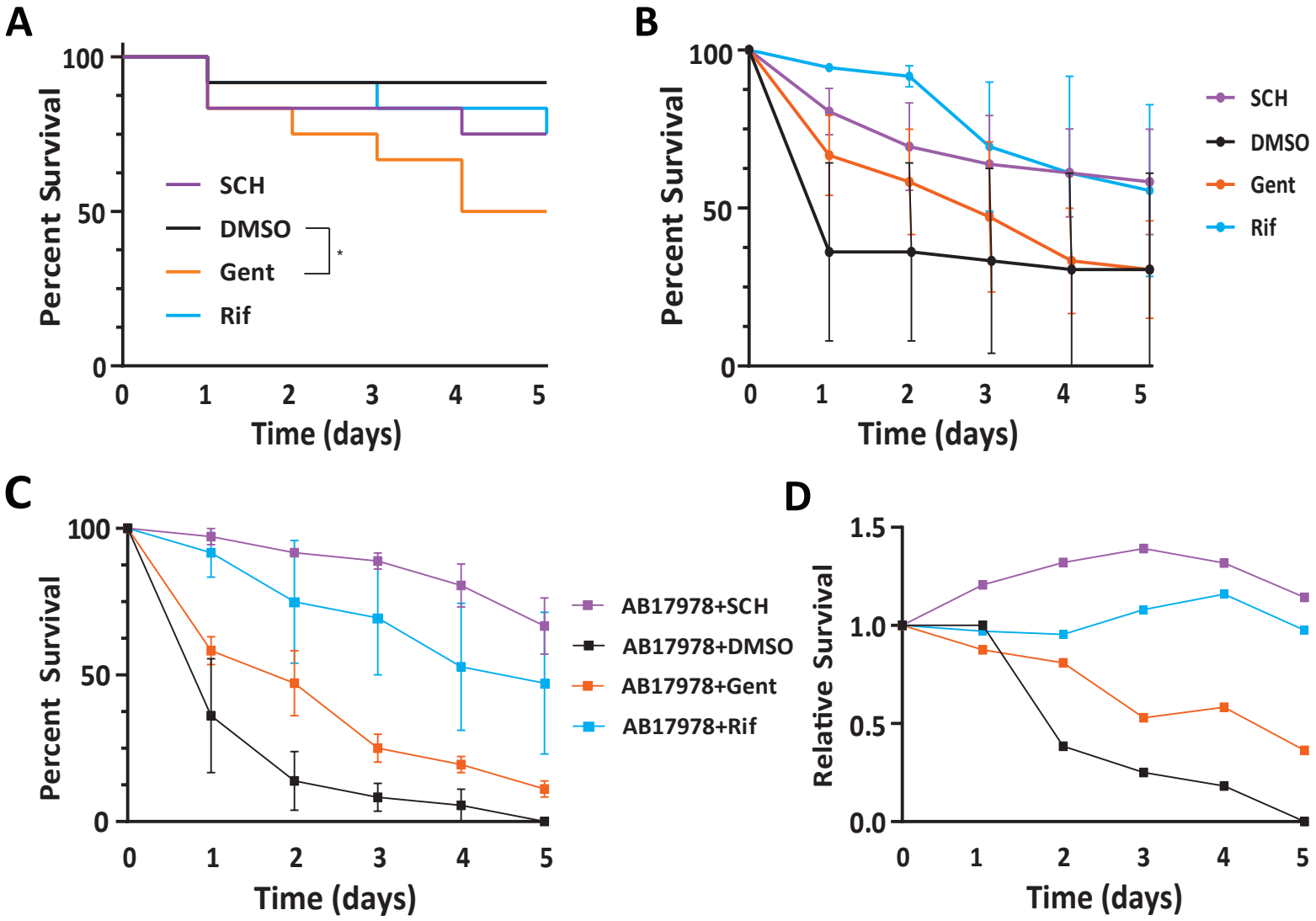

Supplementary Figure 3

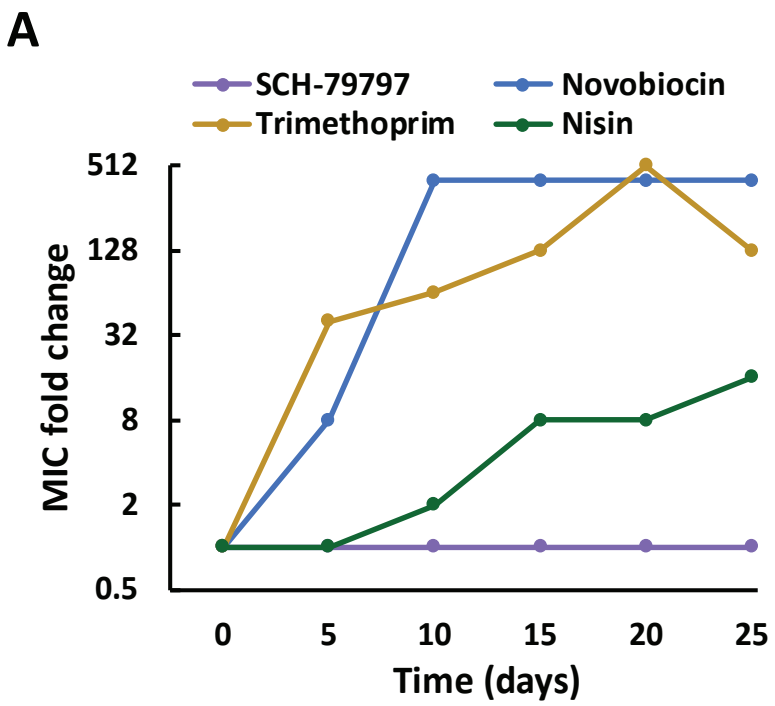

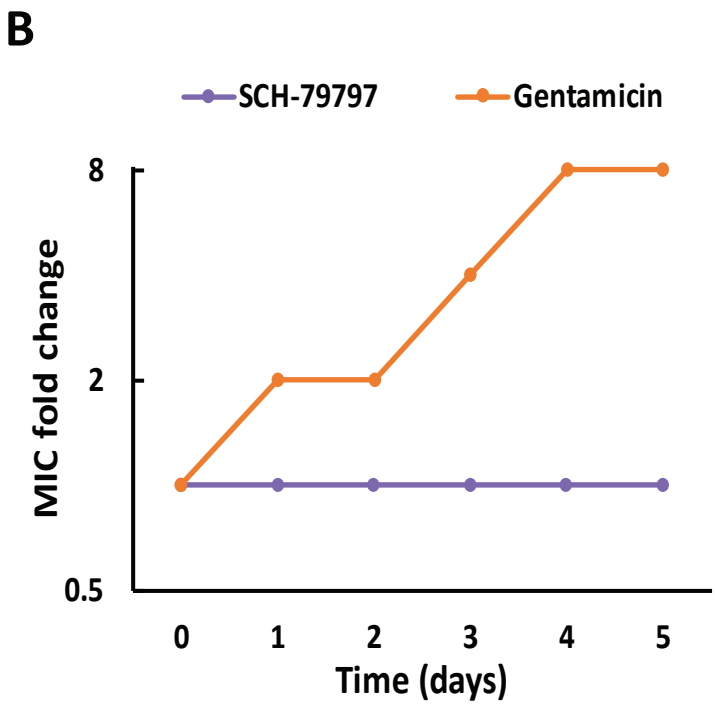

Supplementary Figure 4

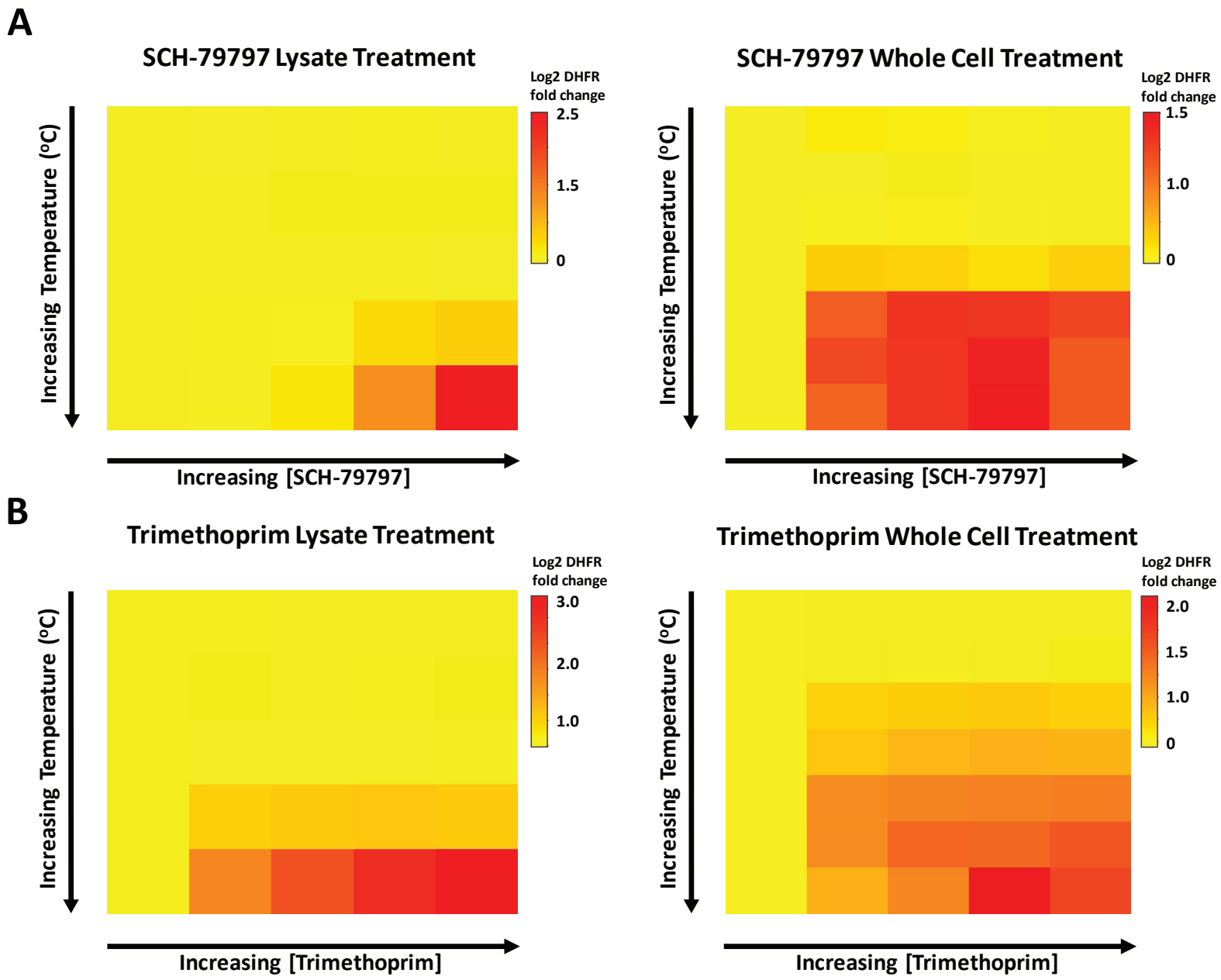

Supplementary Figure 5

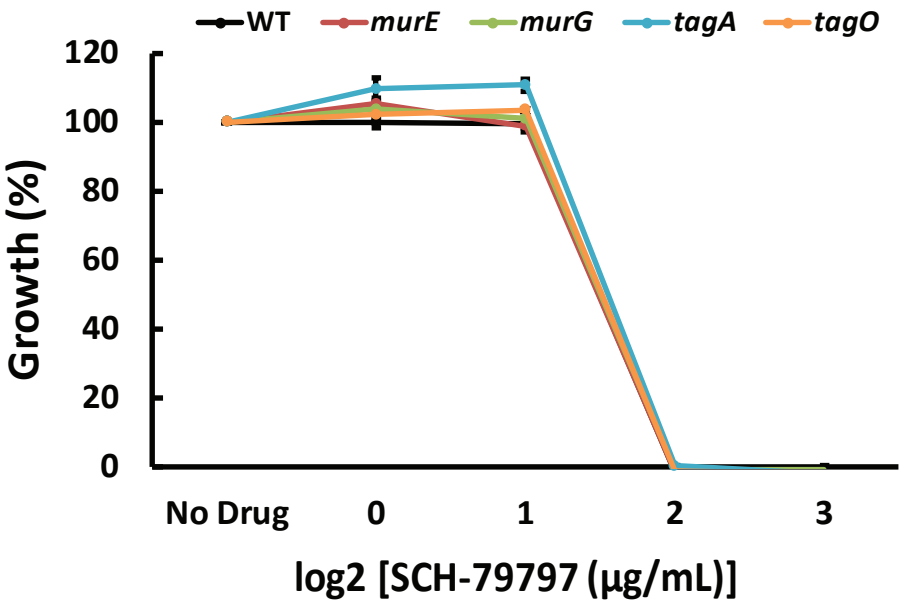

Supplementary Figure 6

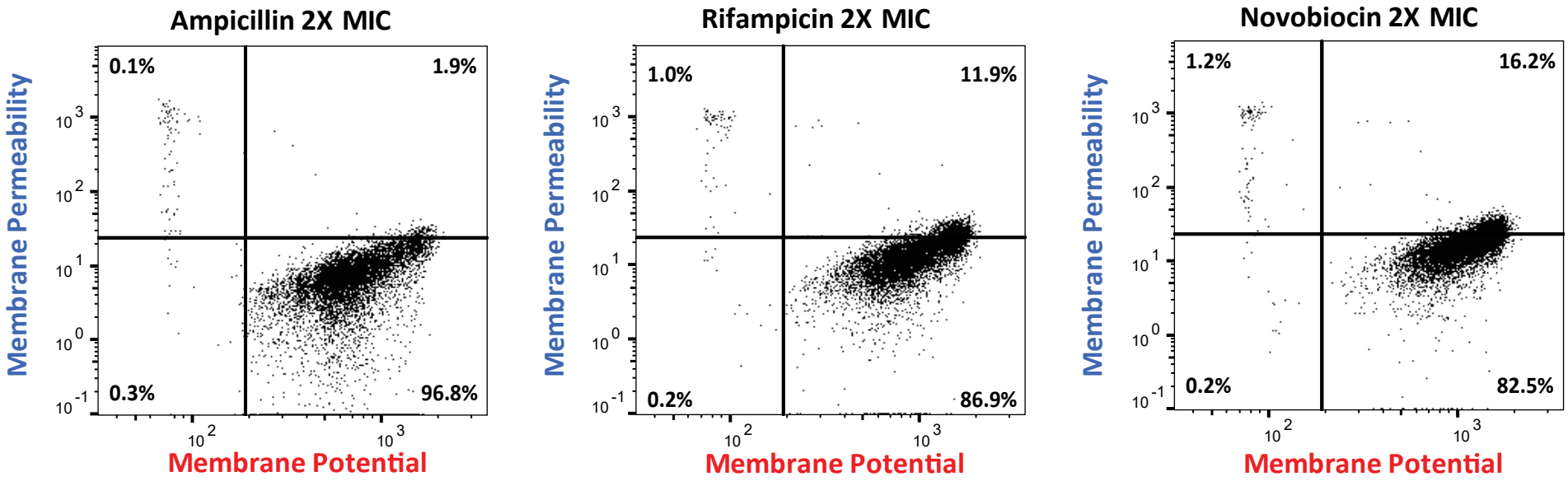

Supplementary Figure 7